Investigation on numeric methods solving heteroclinic trajectories in Hamilton systems

Ziheng Chen

October 31, 2018

1 Example Systems

Here we restrict the topic to Hamiltonian systems, i.e. looking for a solution $(q(t), p(t)), -\infty \leq t \leq +\infty$ such that

$$\begin{cases} \dot{q} &= \dfrac{\partial H}{\partial p} \\ \dot{p} &= -\dfrac{\partial H}{\partial q} \end{cases}, \tag{1}$$

while the boundary conditon is

$$\nabla H(q(-\infty), p(-\infty)) = \nabla H(q(+\infty), p(+\infty)) = 0.$$

1.1 (Generalized) Simple Gradient System

A simple system is proposed as

$$H_1 = \frac{1}{2}p^2 + p\left(q - q^3\right). \tag{2}$$

The analytical solution to Eqn 2 is

$$\begin{cases} q(t) &= -\frac{1}{\sqrt{1+\exp(2t)}} \\ p(t) &= 2\left(q(t)^3 - q(t)\right) \end{cases}.$$

System described by Eqn 2 can be easily extended to higher dimensions, such as

$$H_2 = \frac{1}{2}\sum_{i=1}^{2} p_i^2 + \sum_{i=1}^{2} p_i\left(q_i - q_i^3\right) + \left[\left(q_2^2 - 1\right)q_1^2 - L\left(q_1^2 - 1\right)q_2^2\right]^2, \tag{3}$$

of which the solution is

$$(q_1, q_2, p_1, p_2) = \left(q_2\sqrt{\frac{L}{1+(L-1)\,q_2^2}}, \frac{1}{\sqrt{1+\exp(2t)}}, 2\left(q_1^3 - q_1\right), 2\left(q_2^3 - q_2\right)\right).$$

1.2 Seven-atom hexagonal Lennard-Jones cluster

The system is a gradient one (see [Dellago et al., 1998]), proposed as

$$H = \frac{1}{2}p^T \cdot p + \nabla V^T \cdot p, \tag{4}$$

where

$$V = \sum_{i<j} v(r_{ij}), v(r) \triangleq 4\left(r^{-12} - r^{-6}\right).$$

1.3 Non-gradient System

This system is proposed in [Newman et al., 1990] as

$$H = p_1 \cdot q_2 + p_2 \left[\frac{1}{4} p_2 + f'(q_1) q_2 \right] - (q_2 - f(q_1))^2, \tag{5}$$

where f has at least two roots.

2 Eigenvalue-based method

2.1 Method Description

It is quite obvious that around the steady states $(q(\pm\infty), p(\pm\infty))$, the system described in Eqn 1 can be analyzed in a linearized form.

Suppose the solution can be arclength-parameterized, i.e.

$$S \triangleq \int_{-\infty}^{+\infty} \sqrt{\left(\frac{d}{dt}q\right)^2 + \left(\frac{d}{dt}p\right)^2}\, dt < \infty.$$

Thus a arclength mapping $s(t)$ can be defined as

$$s(t) \triangleq \frac{1}{S} \int_{-\infty}^{t} \sqrt{\left(\frac{d}{dt_1}q\right)^2 + \left(\frac{d}{dt_1}p\right)^2}\, dt_1. \tag{6}$$

We define $\widehat{q}$ and $\widehat{p}$ accordingly:

$$\widehat{q}(s) \triangleq q\left(t^{-1}(s)\right)$$
$$\widehat{p}(s) \triangleq p\left(t^{-1}(s)\right)$$

Suppose the trajectory $(\widehat{q}, \widehat{p})$ is $C^{(1)}$ on $s \in [0,1]$. If we want to investigate how the trajectory is coming out from $(\widehat{q}(0), \widehat{p}(0))$, we can introduce $\delta\widehat{q}(s) = \widehat{q}(s) - \widehat{q}(0), \delta\widehat{p}(s) = \widehat{p}(s) - \widehat{p}(0)$ and observe that

$$\begin{aligned}
\frac{d}{ds}\widehat{q}(s) &= \frac{d}{dt}q(t) \cdot \frac{dt}{ds} \\
&= H_p(q(t), p(t)) \cdot \frac{dt}{ds} \\
&= H_p\left(q\left(t^{-1}(s)\right), p\left(t^{-1}(s)\right)\right) \cdot \frac{dt}{ds} \\
&= \left[H_{pq}(\widehat{q}(0), \widehat{p}(0)) \cdot \delta_0\widehat{q}(s) + H_{pp}(\widehat{q}(0), \widehat{p}(0)) \cdot \delta_0\widehat{p}(s) + \boldsymbol{O}\left(s^2\right)\right] \cdot \frac{dt}{ds}
\end{aligned} \tag{7}$$

and the same goes to $\dfrac{d}{ds}\widehat{p}(s)$:

$$\begin{aligned}
\frac{d}{ds}\widehat{p}(s) &= \frac{d}{dt}p(t) \cdot \frac{dt}{ds} \\
&= -H_q(q(t), p(t)) \cdot \frac{dt}{ds} \\
&= -H_q\left(q\left(t^{-1}(s)\right), p\left(t^{-1}(s)\right)\right) \cdot \frac{dt}{ds} \\
&= -\left[H_{qq}(\widehat{q}(0), \widehat{p}(0)) \cdot \delta_0\widehat{q}(s) + H_{qp}(\widehat{q}(0), \widehat{p}(0)) \cdot \delta_0\widehat{p}(s) + \boldsymbol{O}\left(s^2\right)\right] \cdot \frac{dt}{ds}
\end{aligned} \tag{8}$$

by using the fact that $\nabla H\left(\widehat{q}\left(0\right),\widehat{p}\left(0\right)\right)=0$. If we let $s\to 0$, Eqn 7 and 8 will lead to

$$\lim_{s\to 0}\frac{\delta_0\widehat{q}\left(s\right)}{\delta_0\widehat{p}\left(s\right)}=\lim_{s\to 0}-\frac{H_{pq}\left(\widehat{q}\left(0\right),\widehat{p}\left(0\right)\right)\cdot\delta_0\widehat{q}\left(s\right)+H_{pp}\left(\widehat{q}\left(0\right),\widehat{p}\left(0\right)\right)\cdot\delta_0\widehat{p}\left(s\right)}{H_{qq}\left(\widehat{q}\left(0\right),\widehat{p}\left(0\right)\right)\cdot\delta_0\widehat{q}\left(s\right)+H_{qp}\left(\widehat{q}\left(0\right),\widehat{p}\left(0\right)\right)\cdot\delta_0\widehat{p}\left(s\right)}, \tag{9}$$

which implies that $\lim_{s\to 0}\mathbf{normal}\left(\delta_0\widehat{q}\left(s\right),\delta_0\widehat{p}\left(s\right)\right)=\left(u,v\right)$ is the eigen vector of the following eigen problem:

$$\lambda_0\left[\begin{array}{c}u\\v\end{array}\right]=L_H\left(\widehat{q}\left(0\right),\widehat{p}\left(0\right)\right)\left[\begin{array}{c}u\\v\end{array}\right],L_H\triangleq\left[\begin{array}{cc}\partial_{pq}&\partial_{pp}\\-\partial_{qq}&-\partial_{qp}\end{array}\right]H. \tag{10}$$

For λ_0, the eigenvalue should be the most positive since it dominates the limit in Eqn 9. We can similarly write the according conclusion for the other steady point, which reads

$$\lambda_1\left[\begin{array}{c}u\\v\end{array}\right]=L_H\left(\widehat{q}\left(1\right),\widehat{p}\left(1\right)\right)\left[\begin{array}{c}u\\v\end{array}\right] \tag{11}$$

for $\lim_{s\to 0}\mathbf{normal}\left(\delta_1\widehat{q}\left(s\right),\delta_1\widehat{p}\left(s\right)\right)=\left(u,v\right),\delta_1 f\left(s\right)=f\left(s\right)-f\left(1\right)$, where λ_1 should be the most negative eigenvalue.

2.2 Algorithm

The tricky part is that we don't know S beforehand, so the mapping described in Eqn 6 can only be written as

$$\widetilde{s}\left(t\right)\triangleq\int_{-\infty}^{t}\sqrt{\left(\frac{d}{dt_1}q\right)^2+\left(\frac{d}{dt_1}p\right)^2}dt_1,\widetilde{s}:\mathbb{R}\to\left(0,S\right)$$

with the upper bound S unknown. If we take $\widetilde{s}\left(t\right)$ back into Eqn 1, we can propose the following scheme:

1. Choose a proper starting direction (u,v), which is the eigen solution of Eqn 10. Assign $x_0=\left(u,v\right)\cdot\Delta h+\left(q\left(-\infty\right),p\left(-\infty\right)\right)$.
2. Based on $x_n=\left(\widetilde{q}\left(\widetilde{s}_n\right),\widetilde{p}\left(\widetilde{s}_n\right)\right),\widetilde{s}_n=n\Delta h$, calculate the update direction using an ODE integrator.
3. Determine if x_{n+1} is close to $\left(q\left(+\infty\right),p\left(+\infty\right)\right)$ enough. If not, continue to Step 2.

Now we explain the procedures in detail.

2.2.1 Choice of the Initial Direction

It is clear when $L_H\left(\widehat{q}\left(0\right),\widehat{p}\left(0\right)\right)$ has only one most positive eigenvalue λ_+, while the choice maybe difficult if λ_+ is a multiple eigenvalue. If it is the case, we can have a grid search in the space $\mathrm{Ker}\left(\lambda_+ I-L_H\left(\widehat{q}\left(0\right),\widehat{p}\left(0\right)\right)\right)$ by its coordinate form. More specifically, since our problems are at most 2-dimensional, the eigenspace is at most two dimension, so a line search in the polar coordinate is enough.

2.2.2 ODE Integrator

It is tempting to only use a simple integrator for proof for concept (like forward Euler), but since we are dealing with Hamiltonian systems, we should better preserve the hamiltonian, which can be achieved if we use symplectic schemes (like Mid-point Euler with estimation-correction).

2.2.3 Stop Criterion

Notice that $\lim_{s\to 0}$ **normal** $(\delta_1 \widehat{q}(s), \delta_1 \widehat{p}(s))$ is an eigen solution to Eqn 11 with negative eigenvalue, so in general any numerical error will be greatly magnified when $s \to S$, pushing the numerical solution onto the unstable manifold around $(q(+\infty), p(+\infty))$. A way to stop the integration at a proper time is to check the distance between x_n and the steady point $(q(+\infty), p(+\infty))$. If the distance is small enough (less than a given torlerance), we can accept the trajectory and stop the integration.

2.3 Numerical Experiments

Here we demonstrate the solution obtained by carrying out the algorithm described in 2.2. The first problem is tested, results shown in Fig 1 and 2. As least for this simple problem this method fits quite well, and the overall error (estimated from $\max|H|$) can be controlled by decreasing the step used in the integrator. Since we are using symplectic schemes, the hamiltonian is well preserved.

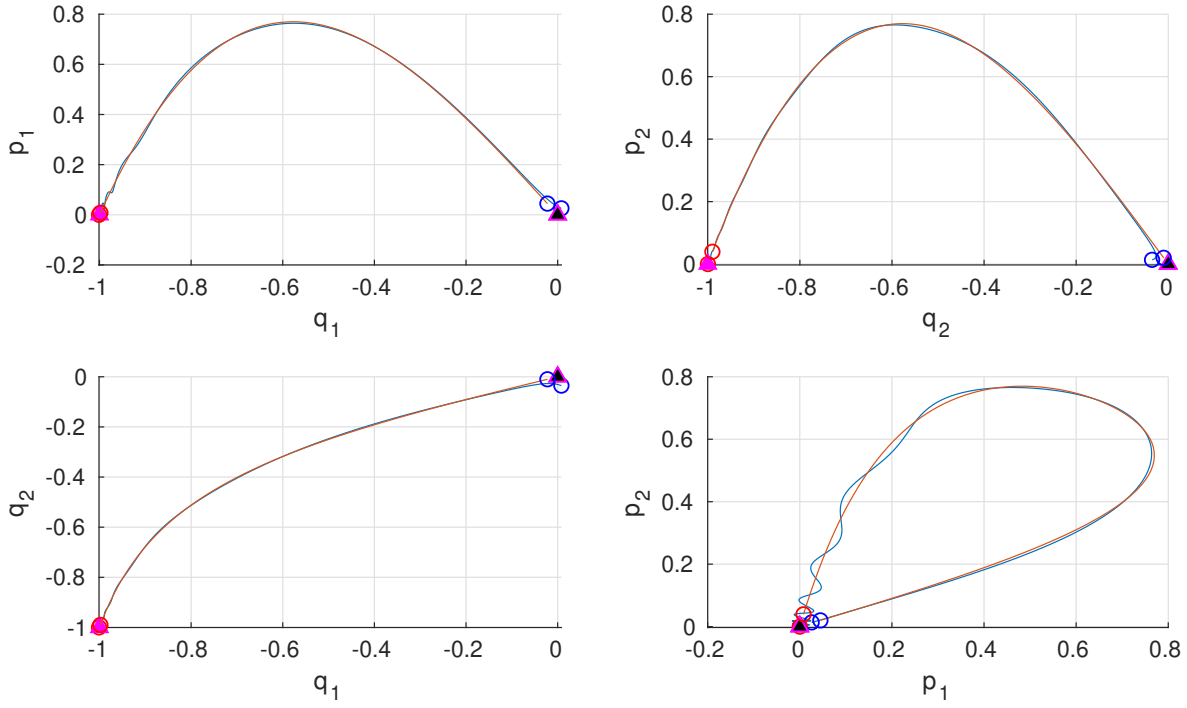

Figure 1: Solution obtained numerically(blue line) and analytically(red line). Notice that the solution starts to be unstable when reaching $s \to 1$(red circle).

However in general, this eigenvalue-based method is not quite as stable as it is shown in the previous example. It is very likely caused by the illposedness near the steady points, where the hamiltonian can change drastically.

3 PDE-based method

3.1 Method Description

The PDE-based method comes from an observation that, if the system is merely more than a gradient system, i.e.

$$H = \frac{1}{2} p^T p + b(q)^T p + l(q), b = \nabla V,$$

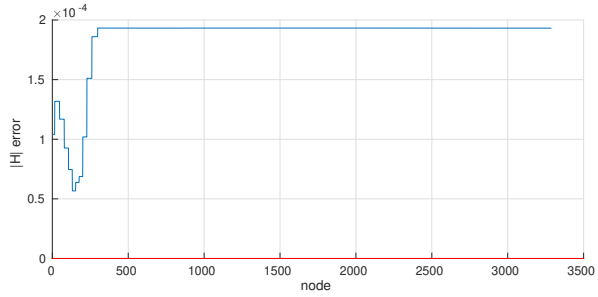

Figure 2: Estimating the error by measuring $|H|$.

which leads to

$$\begin{cases} \dot{q} &= \dfrac{\partial H}{\partial p} = p + b \\ \dot{p} &= -\dfrac{\partial H}{\partial q} = -\left((\nabla b)^T p + \nabla l \right) \end{cases}, \tag{12}$$

we can explicitly solve p by the first line in Eqn 12 and take that into the second line, giving

$$\left(\nabla b - \nabla b^T \right) \dot{q} = \ddot{q} - \nabla b^T \cdot b + \nabla l.$$

But if we are only dealing with gradient systems, i.e. $b = \nabla V$, the vector gradient $\nabla b = \Delta V$ will be symmetric. In this sense, we are looking for a solution to the second-order ODE

$$0 = \ddot{q} - \nabla b^T \cdot b + \nabla l. \tag{13}$$

Actually the solution to Eqn 13 is exactly a non-moving travelling wave solution to the following PDE:

$$\partial_t q = \partial_x^2 q - \nabla b^T \cdot b + \nabla l. \tag{14}$$

Eqn 14 is also known as a reaction-diffusion equation, which is a "heat equation" with a reaction term $-\nabla b^T \cdot b + \nabla l$. Since Eqn 14 acts locally like a heat equation, it also shares some nice features such as smoothness of the solution.

3.2 Algorithm

Most of the work below is on how to correctly solve the PDE in Eqn 14. Except the reparameterization method, we suppose that $q(x,t)$ is discretized on the grid of grid $(-A, A, h) \times$ grid $(0, T, \tau)$, where grid(l, r, δ)=$\{l, l+\delta, \dots r-\delta, r\}$.

3.2.1 Boundary Conditions

There are roughly two conditions to choose: Dirichlet and Neumann condition.

- Dirichlet condition: $q(-A,t) = q_{-\infty}, q(+A,t) = q_{+\infty}$.
- Neumann condition: $\partial_x q(-A,t) = \partial_x q(+A,t) = 0$.

3.2.2 Update Scheme

We included the following three schemes (denoting $f(q) \triangleq -\nabla b^T \cdot b + \nabla l$)

- Forward Euler (explicit scheme):

$$\frac{\Delta_{+\tau}}{\tau}(q(x,t)) = \frac{\delta_h^2}{h^2}(q(x,t)) + f(q(x,t)). \tag{15}$$

- Backward Euler (implicit scheme):

$$\frac{\Delta_{+\tau}}{\tau}\left(q\left(x,t\right)\right)=\frac{\delta_h^2}{h^2}\left(q\left(x,t+\tau\right)\right)+f\left(q\left(x,t+\tau\right)\right).$$

- Crank-Nicolson (implicit scheme):

$$\frac{\Delta_{+\tau}}{\tau}\left(q\left(x,t\right)\right)=\frac{1}{2}\left[\frac{\delta_h^2}{h^2}\left(q\left(x,t\right)\right)+f\left(q\left(x,t\right)\right)+\frac{\delta_h^2}{h^2}\left(q\left(x,t+\tau\right)\right)+f\left(q\left(x,t+\tau\right)\right)\right].$$

3.2.3 Stop Criterion

Since we are interested in finding a path that preserves $H=0$, it is convincing to use $\left|H\left(q\left(\xi\right),p\left(\xi\right)\right)\right|_\infty$ as an indication if $q\left(x,t\right)$ is close to $q_0\left(\xi\right)=q\left(\xi,\infty\right)$ enough. To obtain H, we have to obtain $p\left(\xi\right)$ by

$$p\left(\xi\right)=\dot{q}\left(\xi\right)-b\left(q\left(\xi\right)\right). \tag{16}$$

A tricky thing is that Eqn 16 is directional, i.e. $q\left(-\xi\right)$ will not give the correct $p\left(\xi\right)$, so we should know which direction the trajectory is (it is also quite important in the original system).

3.2.4 Change in coordinate

Still Eqn 14 contains infinite range for x, which introduces quite a lot truncation error; which is worse is that on most of the nodes the solution $q\left(x,t\right)$ is quite "flat". A way to work around is to change the space coordinate x into another finite range coordinate y. One feasible mapping is the arctan function:

$$\mathring{q}\left(y,t\right)\triangleq q\left(\tan\left(x\right),t\right).$$

To tranform Eqn 16 into coordinate (y,t), we should eliminate x by chain rules:

$$\frac{\partial}{\partial y}\mathring{q}=\left(\frac{\partial}{\partial x}q\right)\cdot\left(\frac{dx}{dy}\right),$$

$$\frac{\partial^2}{\partial y^2}\mathring{q}=\left(\frac{\partial^2}{\partial x^2}q\right)\cdot\left(\frac{dx}{dy}\right)^2+\left(\frac{\partial}{\partial x}q\right)\cdot\left(\frac{d^2x}{dy^2}\right),$$

so if we combine the two equations above

$$\begin{aligned}\frac{\partial^2}{\partial x^2}q&=\left(\frac{\partial^2}{\partial y^2}\mathring{q}\right)\cdot\left(\frac{dy}{dx}\right)^2-\left(\frac{\partial}{\partial y}\mathring{q}\right)\cdot\left(\frac{d^2x}{dy^2}\right)\cdot\left(\frac{dy}{dx}\right)^3\\&=\left(\frac{\partial^2}{\partial y^2}\mathring{q}\right)\cos^4\left(y\right)-2\left(\frac{\partial}{\partial y}\mathring{q}\right)\sin\left(y\right)\cos\left(y\right)^3.\end{aligned} \tag{17}$$

Then we can apply the discussions occured in the previous subsubsections onto the tranformed PDE (Eqn 17).

3.3 Numerical Experiments

3.3.1 On Generalized Simple Gradient System

First we should compare the two boundary conditions. Fig 3 shows the error in $\left|H\right|_\infty$ as t grows. From the figure it is clear that the two boundary conditions act almost the same. Since neumann boundary conditions are much easier to implement, we will always use that in the following experiments. This also shows that the pde-based method is at least feasible.

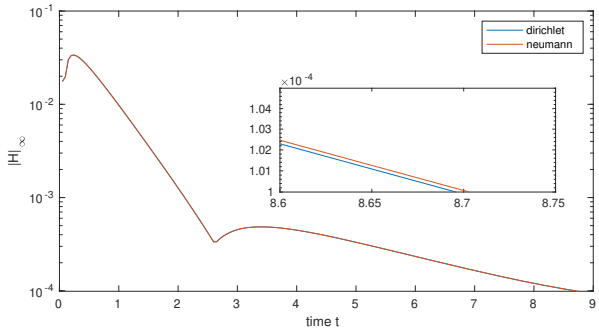

Figure 3: ∞-norm error in the hamiltonian. Inset: a close look at where the stop criterion is about to be statisfied. The x-domain is grid $(-6, 6, 1/16)$.

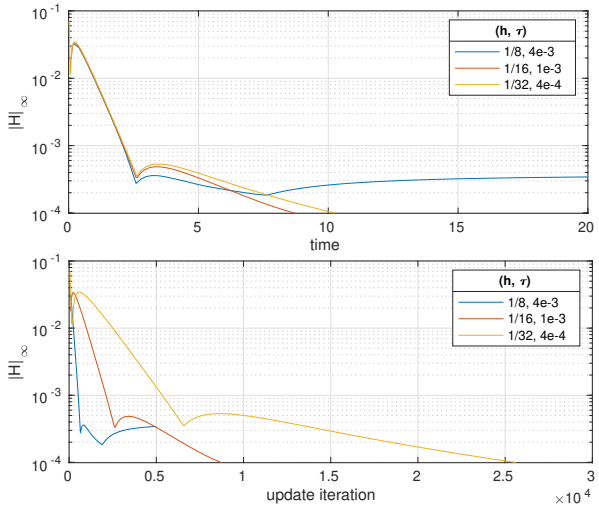

Figure 4: ∞-norm error in the hamiltonian when using different space discretization step.

A next question is that if the space resolution is enough, i.e. if the h in grid $(-6, 6, h)$ matters. Fig 4 shows the comparison between different (h, τ) settings. It is quite clear that $h = \frac{1}{8}$ is not precise enough and introduces some artificial errors, while $h = \frac{1}{16}, \frac{1}{32}$ gives similar results. But from Fig we can see that $h = \frac{1}{16}$ uses much fewer iterations, for smaller space step needs accordingly small time step.

Then we should compare if there is any improvement to use implicit update scheme since every step it requires solving a non-linear system. We will all use $h = \frac{1}{16}$ for space discretization.One thing worth noticing is that to make sure implicit methods are stable, we should run explicit methods beforehand to make the initial boundary value close to the possibly desired solution.

Finally we want to investigate if a change in the space coordinate can really help to solve the system. Fig 6 shows how the remaining error $|H|_\infty$ decreases as the algorithm iterates. Although Eqn 17 requires more calculation (like $\cos(y)^4$) compared to the straight forward one (Eqn 14), we can actually use less nodes to achieve almost the same precision (see Fig 7 and 8).

3.3.2 On a seven-atom hexagonal Lennard-Jones cluster

First we have to obtain the correct relative positions for each atom, which is obtained by solving an optimization problem, given a hexagonal-positioning initial guess. Then we use the same algorithm

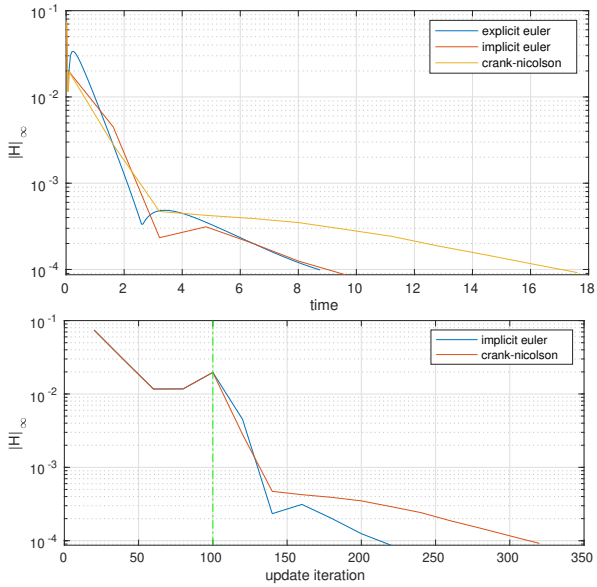

Figure 5: ∞-norm error in the hamiltonian when using different update schemes. Green dashed line indicates that we assume the solution is close enough so that implicit method can take on over explicit methods.

introduced above to compute the trajectory between each two configurations. A tricky thing is that we cannot know the rotation beforehand (it is obvious that the whole system should not have any non-zero angular momentum at any time), and any rotated steady configuration is also a steady configuration, so there maybe a net rotation after the transition, which is ill-posed to some extent. For numerical solutions, we refer to Fig 9, 10 and 11.

References

[Dellago et al., 1998] Dellago, C., Bolhuis, P. G., and Chandler, D. (1998). Efficient transition path sampling: Application to lennard-jones cluster rearrangements. *The Journal of Chemical Physics*, 108(22):9236–9245.

[Newman et al., 1990] Newman, T. J., Bray, A. J., and McKane, A. J. (1990). Inertial effects on the escape rate of a particle driven by colored noise: An instanton approach. *Journal of Statistical Physics*, 59(1):357–369.

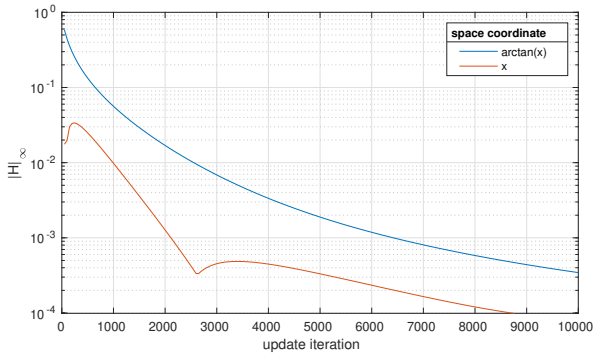

Figure 6: Comparison between two space coordinates choices. A change in space coordinate does require more calculation, but we can use less nodes and achieve faster speed (0.694s compared to 0.726s when there is no such change).

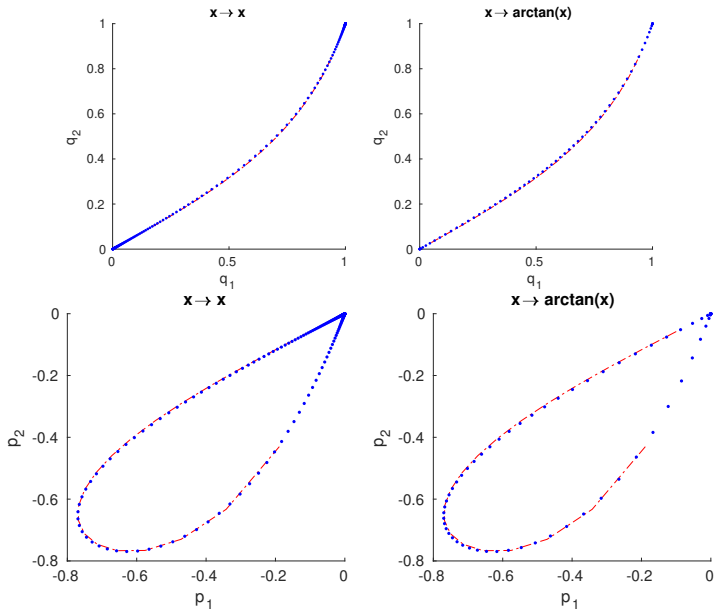

Figure 7: Comparison between solution obtained under different space coordinate settings. Red dashed line indicates the analytical solution. Nodes on the right side plots are much separated.

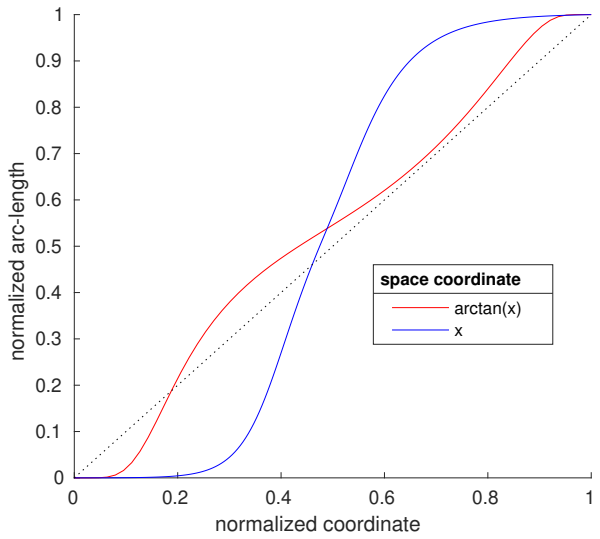

Figure 8: Relation between normalized space coordinate and normalized arc-length. Back dotted line indicates perfect arc-length parameterization.

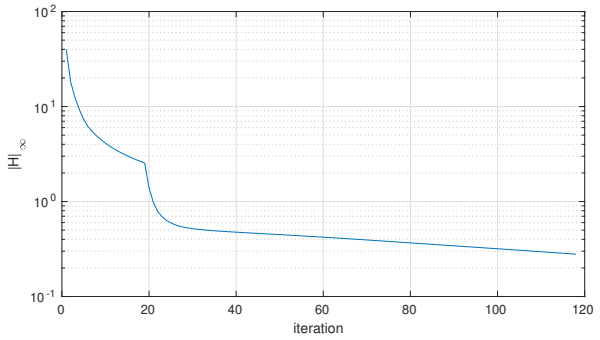

Figure 9: ∞-norm error in the hamiltonian. $(h, \tau) = \left(\frac{1}{8}, 10^{-5}\right)$, time update scheme: explicit Euler. Total time used for 2000 iterations: 75.80s.

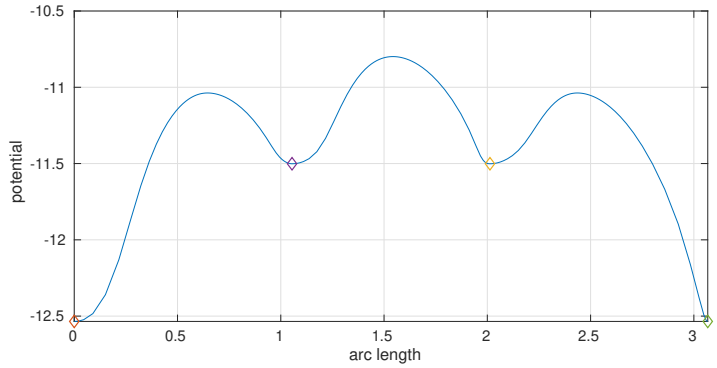

Figure 10: Potential changing along the arc length parameter. From left to right: A(red), B(purple), C(yellow), D(green).

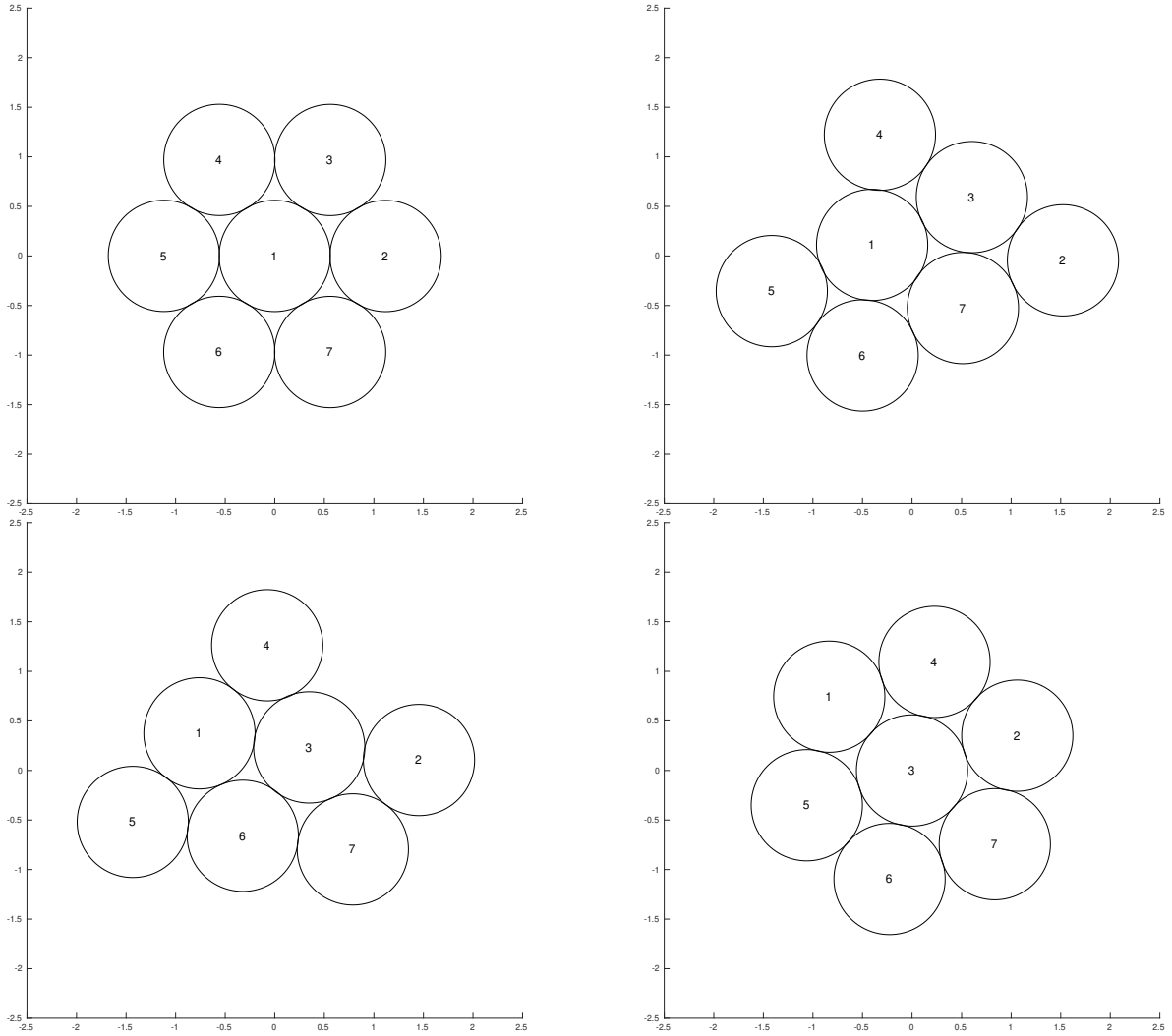

Figure 11: From left to right, top to bottom: configuration A(left-top), B(right-top), C(left-bottom), D(right-bottom).